

Investigation and Characterization of Maghemite ($\gamma\text{-Fe}_2\text{O}_3$) Nanoparticles and Its Cytotoxicity Studies

Mahdi Khodabakhshi, Ali Bahari

¹Department of Physics, Faculty of Basic Sciences, University of Mazandaran, Babolsar, IRAN.

ABSTRACT

Objective: The expansion of wet chemical method for the synthesis of iron oxide nanoparticles with magnetic properties is reported. **Methods:** Iron oxide nanoparticles were investigated in the procedure using Transmission Electron Microscopy (TEM). It has been seen that the distribution size changed by changing of Molarity precursor and heating the sample. The magnetization evaluations were performed using a Vibrating Sample Magnetometer device (VSM) to specify the magnetic answer. The Thermo Gravimetric Analyses (TGA) displayed the size-dependent weight loss of the magnetic nanoparticles. In this work, the cytotoxic activity of various samples of Maghemite on cancer cell lines HELA was studied. The *in vitro* cytotoxicity tests were also performed to determine the cell viability as a work of size and heat of the magnetic nanoparticles. **Results:** The samples c and d at $T = 300^\circ\text{C}$ had a little magnetic hysteresis that can use in cancer cure with hyperthermia therapy method. **Conclusions:** These samples became amorphous and they were nontoxicity.

Key words: Magnetic properties, Maghemite, Iron oxide nanoparticles, Cell viability, Cytotoxicity.

INTRODUCTION

The iron oxide nanoparticles have been widely studied for medical imaging, drug targeting, biomolecule separation,¹ and catalytic applications owing to their unique electrical, magnetic and chemical properties.²⁻⁴ $\gamma\text{-Fe}_2\text{O}_3$ (mineralogically known as maghemite) is the second most common Fe_2O_3 polymorph in nature and can be formed by a wide range of reactions. Like $\alpha\text{-Fe}_2\text{O}_3$, it exists in both bulk and nanosized forms. Maghemite possesses a cubic crystal structure of an inverse spinel type and crystallizes in the P4132 space group with $a = 8.351 \text{ \AA}$.

$\gamma\text{-Fe}_2\text{O}_3$ has a spinel structure with two magnetic sublattices so it is a typical ferromagnetic material like Fe_3O_4 ; it is readily magnetized and thus has a high magnetic response when it is placed in an external magnetic field. Ultrafine particles of $\gamma\text{-Fe}_2\text{O}_3$ (i.e., those with sizes of $\sim 10 \text{ nm}$ or less) exhibit superparamagnetic relaxation. In fact, $\gamma\text{-Fe}_2\text{O}_3$ was one of the materials that

prompted the development of the theory of superparamagnetism, and it has been studied extensively in this context. Superparamagnetism is a thermally activated relaxation phenomenon that is typically observed in nanoscale structures, in which the particle's overall magnetic moment (i.e., superspin) spontaneously fluctuates between various orientations that are energetically favored by its magnetic (magnetocrystalline in most cases) anisotropy. Nanosized $\gamma\text{-Fe}_2\text{O}_3$ is a very useful material in nanotechnological applications because its nanoparticles have interesting magnetic and surface properties and it is nontoxic, biodegradable, biocompatible, and chemically stable⁵ It is really important to get monodispersity during the fabrication of the nanoparticles to increase the sensitivity of these particles for the diverse applications. Hence, the development of novel methods has been the focus of recent research to make uniform and

Submission Date: 30-08-2016;

Revision Date: 17-11-2016;

Accepted Date: 23-11-2016

DOI: 10.5530/ijper.51.2.35

Correspondence:

Mahdi Khodabakhshi,
University of Mazandaran,
Babolsar, IRAN.
Phone no: +989112541439
E-mail: khp.mahdi@gmail.
com



www.ijper.org

highly monodispersed nanoparticles by the wet chemical method,^{6,7} and the thermal decomposition method. However, there are not many reports on detailed studies of the growth process of monodispersed superparamagnetic iron oxide nanoparticles (SPIONs), although the syntheses of relatively uniform magnetite and maghemite nanoparticles have been reported.⁸

It was observed that the wet chemical method for iron oxide nanoparticles is advantageous since it was a method to produce under 10 nm particles.⁹ SPION that are 10-100 nm in size are considered to be optimal for intravenous administration whereas particles >200 nm and <10 nm are sequestered by the spleen or removed through renal clearance, respectively.¹⁰

However, properties of SPION govern their ultimate fate in terms of the efficiency of cellular uptake, bio distribution, metabolism and potential toxicity. The purpose of the present investigation is to study the size distribution of the particles as well as the iron oxide nanoparticles during process since it is not studied in detail before. We tried to investigate applications of magnetic nanoparticles and found good samples in medical applications. We tried to find particles with small size and synthesis of γ phase of Fe_2O_3 . The toxicity of nanoparticles and their effects on alive cells were investigated, too. The iron oxide nanoparticles were characterized by X-ray diffraction (XRD), thermo gravimetric analysis (TGA), Transmission electron microscopy (TEM) and vibrating sample magnetometer (VSM). The synthesis of iron oxide nanoparticles was found to be reproducible with the tunable properties. The *in vitro* cell viability tests were also performed for these iron oxide nanoparticles to determine their cytotoxic effects.

MATERIALS AND METHODS

Synthesis of Iron Oxide Nanoparticles

The nanoparticles were prepared by following a procedure reported in the literature.⁷ The synthesis procedure was as follows: FeCl_3 and $\text{FeCl}_2 \cdot 4\text{H}_2\text{O}$ were dissolved in a 2M hydrochloric acid to form a solution with the concentration of 1M for FeCl_3 and 2M for $\text{FeCl}_2 \cdot 4\text{H}_2\text{O}$. The $\text{NH}_3 \cdot \text{H}_2\text{O}$ solution (2M) was added drop by drop to this solution with vigorous stirring at room temperature for 2 h. The final pH of this solution was 9.73. Then put it in centrifuges with 5000 rpm for 10 minutes. This precipitate was then collected by filtration and rinsed three times with deionized water and ethanol. Finally, the washed precipitate was dried at 70°C overnight. In the second test, the molarity of FeCl_3 solution and

FeCl_2 solution was respectively changed to 2 molar and 3 molar, sample (b). The powders (samples (a) and (b)) were heated in temperature 300°C for three hours (according to the TGA analysis) and were called samples (c) and (d), respectively.

Cytotoxicity Assay

Considering the increasing applications of the magnetic nanoparticles in the biomedical fields, the *in vitro* cell viability studies were performed in the presence of the maghemite nanoparticles synthesized by the above method.^{11,12} The Cervical cancer cells (HELA) were used for cytotoxicity tests.¹³ These cells (104 cells per 100 μl Culture medium) of different concentrations of nanoparticles (in 0, 1, 50, 100, 500, 1000 $\mu\text{g/mL}$) were seeded into different wells and were incubated for 48 h followed by the addition of 20 mL of MTT (methyl thiazolyl tetrazolium) in each well and incubated for 4 hours. Then, MTT solution was excluded from wells, and 50 μl of DMSO was added to each well and the 96 well/plates were shaken for 15 minutes. At the end, the absorbance was determined by ELISA reader ($\lambda_{\text{max}} = 490$ and 630 nm).^{14,15}

Characterization

Direct structural and size information of magnetic nanoparticles has been analyzed by using transmission electron microscopic analysis with specifications (Zeiss - EM10C - 80 KV).

The crystallographic structure of the sample was analyzed by powder X-ray Diffractometer with $\text{CuK}\alpha$. The XRD data was collected by step scanning over the angular range of $20^\circ \leq 2\theta \leq 80^\circ$, at room temperature, 30% humidity. The average size of nano-crystals was calculated by Scherrer's formula according to Eq.(1). Since the Scherrer equation has been used for measuring the size of spherical crystallites, we used the X-powder software¹⁶ to calculate the particles' size. This software calculated with Scherrer equation (Eq. 1).

$$\text{Eq.(1)} \quad D = \frac{0.89 \lambda}{\beta \cos \theta}$$

Where D is the nanoparticles size in nm, λ (Wavelength of X-Rays) = 0.15406 nm, β maximum peak width at half of the height in radians and θ is diffraction angle of the highest peak in degrees.

To determine the magnetic behavior of synthesized powder, VSM technique it has been used. The vibrating sample magnetometer (VSM) was used to measure magnetic properties of the samples at room temperature. The composition of nanoparticles was determined by thermo gravimetric analysis (TGA).

RESULTS AND DISCUSSION

TEM

In wet chemical method, the nanoparticle formation involves steps mainly making solution, combined dilution, drying and powdering. To understand size of nanoparticles, TEM images were obtained. TEM images of iron oxide nanoparticles for sample (a) have been shown (in the Figure 1, panel (a)). In this method the size of nanoparticles was about 3 nm with a narrow size distribution. After calcining at 300°C for three hours, (sample (c)) it was observed that the size of distribution became bigger but the majority of nanoparticles still possessed the average size of 6 nm, which is (shown in Figure 1), panel (c). The mediocre of size distribution was seen in the sample (b) that shifted to 4 nm (as shown in Figure 1, panel (b)). When the nanoparticles were calcined at 300°C for three hours, the size distribution became longer and more narrow (as shown in Figure 1, panel (d)) (with the average size of 9 nm).

XRD

Figure 2 panel (I) shows the XRD patterns of iron oxide Nano crystals of the standard $\gamma\text{-Fe}_2\text{O}_3$. The peak positions and relative intensities of nanoparticles were well agreed with XRD patterns of standard $\gamma\text{-Fe}_2\text{O}_3$, which confirms the obvious inverse spinel structure of the maghemite materials. Figure 2 panel (II) shows that nanoparticles have been got amorphous after heating, only the (311) plan has a high peak. The average sizes of the iron oxide nanoparticles were calculated from Scherer's equation as given in Table 1, which was consistent with the result obtained from the transmission electron microscopy (TEM) analysis.

All diffraction peaks in Figure 2 are consistent with the standard structure of maghemite (JCPDS card No. 39-1346).

TGA

The weight loss in TG analysis for iron oxide nanoparticles is shown in Figure 3. The TGA curve displays a weight loss from room temperature to 250°C and a drop between 250-400°C, respectively. The weight loss in the low-temperature region is resulted from evaporating of free hydrochloric acid and the H_2O . However, the weight loss at relatively high temperatures can be attributed to the decomposition of hydrochloric acid bound to the nanoparticles. The decomposition at higher temperatures can be attributed to the chemical bonding between iron and the carbonyl group. Since the smaller nanoparticles provide more binding sites on the surface

for surfactant than larger ones, the amount of weight loss is related to the particle size due to the higher surface area to volume ratio of nanoparticles (shown in Figure 3).

VSM

A vibrating sample magnetometer (VSM) was used to measure magnetic properties of the samples at room temperature. The applied magnetic field was between -8500 to 8500 Oe.

Figure 4 (I) shows the magnetization curves of samples $\gamma\text{-Fe}_2\text{O}_3$ at room temperature. Sample (a) and sample (b) show superparamagnetic behavior with zero coercivity and remanence. The shape of the hysteresis loop is depended on particle size. When the particle size decreases, the number of magnetic domains per particle decreases down to the limit where it is energetically unfavorable for a domain wall to exist. Below a critical diameter (below 5 nm), the magnetic particles have a single domain; the particles are then superparamagnetic. The superparamagnetic nanoparticles fluctuate due to thermal energy, this fluctuation tends to randomize the moments of the nanoparticles unless a magnetic field is applied, at this condition coercivity is negligible.¹⁷ This is related to the fine crystallite sizes of $\gamma\text{-Fe}_2\text{O}_3$ particles, which are in the range of 2 – 5 nm¹⁸ nanoparticle characterization is typically performed under the pretext of well-dispersed, aqueous conditions. Here, we systematically characterize the effects of aggregation on the alternating magnetic field induced heating and magnetic resonance (MR).

The M-H curve was measured for samples (c) and (d) at room temperature and the results are shown in Figure 4 (II). It was obvious in the figure that magnetic saturation for samples a and b happened at 4000 Oe external field and external field of 1000 Oe for samples c and d. That showed good distribution and crystalline of maghemite nanoparticles. Magnetic saturation of samples a and b was about 35 and about 5 for samples c and d. It was very different from the magnetic saturation of bulk maghemite (~ 72).^{19,20} The results showed that the magnetic saturation increased with decreasing the particles' size. As the magnetic hysteresis of samples a and b was 0, it confirmed the superparamagnetic properties of these samples. But samples c and d had a little magnetic hysteresis so these samples could be ferromagnetic. The coercivity and magnetic saturation of samples c and d were a little. The samples at $T=300^\circ\text{C}$ did not have any magnetic dipoles of O ions and dipoles of iron oxides were in different directions. As we can

see in Figure 4 (I) the coercivity magnetic was 0 for zero magnetic field. These samples were antiferromagnetic. As the hysteresis loops of samples a and b were 0, the magnetic nanoparticles of Fe γ phase can correct the carrying of drugs by carrying of medicinal elements and magnetic field.

In Figure 4 (II) for samples c and d, there was a little hysteresis so these samples can use in cancer cure with Hyperthermia therapy method.

The measurements carried out by VSM are consistent with the standard deviation calculated by TEM images.

MTT assay

Common to all NPs, SPION are associated with unique physico-chemical features, such as nanometer sizes and a large surface area to mass ratio that also facilitate novel applications. On the other hand, the same nan scale properties (e.g. large surface area coupled with enhanced reactivity, increased propensity to diffuse across biological membranes, and tissue barriers due to nano-size which causes cellular stress) can potentially induce cytotoxicity that can manifest itself by impairing the functions of the major components of the cell, namely mitochondria, nucleus and DNA.^{21,22} In fact, exposure to SPION has been associated with significant toxic effects such as inflammation, the formation of apoptotic bodies, impaired mitochondrial function

(MTT), membrane leakage of lactate dehydrogenase (LDH assay) generation of reactive oxygen species (ROS), increase in micronuclei (indicators of gross chromosomal damage; a measure of genotoxicity), and chromosome condensation.²³

For analyzing the biocompatibility, the hydrophilic nanoparticles of samples (a), (b), (c) and (d) in the concentrations range of 0, 1, 50, 100, 500 and 1000 mg/ μ l were treated with the Cervical cancer cells (HELA) for 48 h. Figure 5 shows the cell viability results for normal as well as Cervical cancer cells with samples (a), (b), (c) and (d) nanoparticles. The cytotoxicity studies revealed that there is no obvious change in cell viability in the studied concentration range of magnetic nanoparticles, although the 100 μ m nanoparticle concentration is considered to be far higher than the normal use. Thus, as-prepared nanoparticles showed biocompatibility and nontoxicity against the normal as well as cancerous cell lines.

CONCLUSIONS

In summary, we synthesized the iron oxide nanoparticles with monodispersity using the wet chemical method. The magnetic nanoparticles showed well-defined superparamagnetic and blocking temperature due to the size effects consistent with the TEM images. The TG

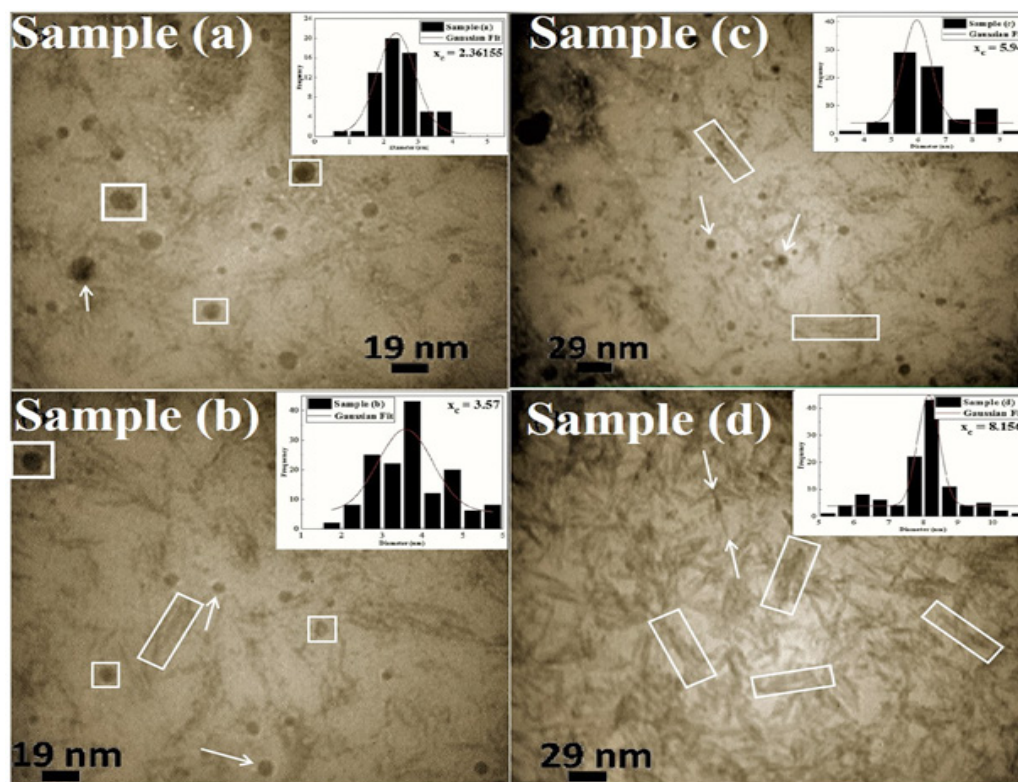


Figure 1: TEM schematic images of samples (a), (b), (c) and (d), and their histograms of size distributions are given in panels (a), (b), (c) and (d) respectively.

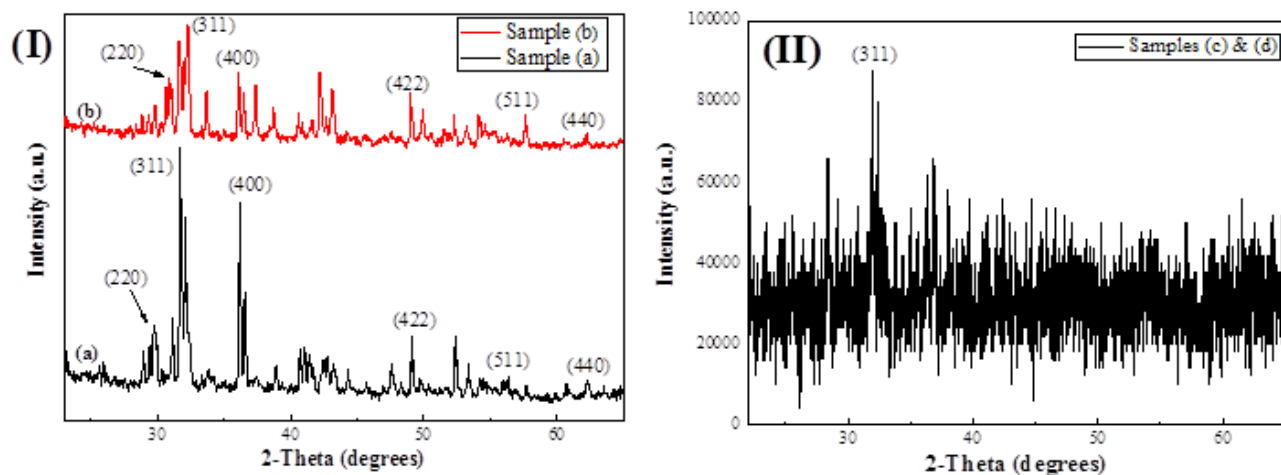


Figure 2: XRD patterns of iron oxide nanocrystals of samples (a), (b), (c) and (d).

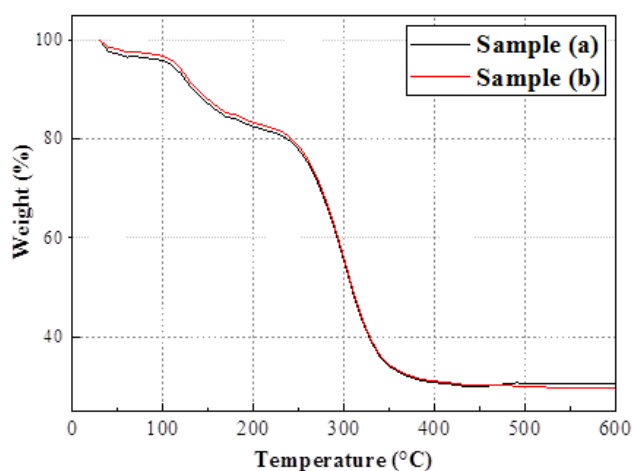


Figure 3: TGA curves of $\gamma\text{-Fe}_2\text{O}_3$ (samples (a) and (b)).

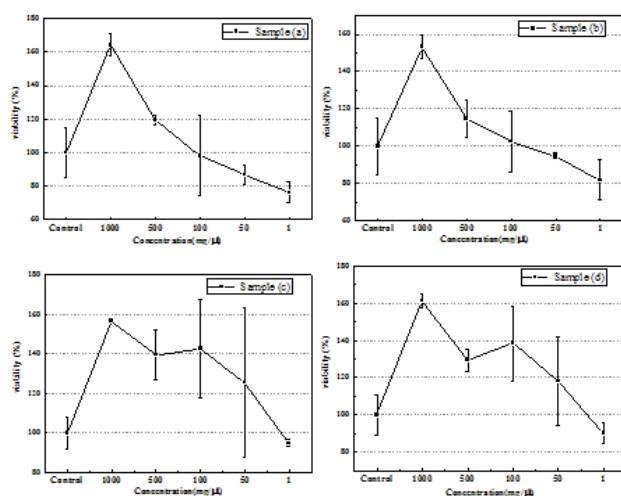


Figure 5: The cytotoxicity tests for Cervical cancer cells (HELA), superparamagnetite iron oxide nanoparticles of samples (a), (b), (c) and (d) in the concentrations range of 0, 1, 50, 100, 500 and 1000 mg/ μl .

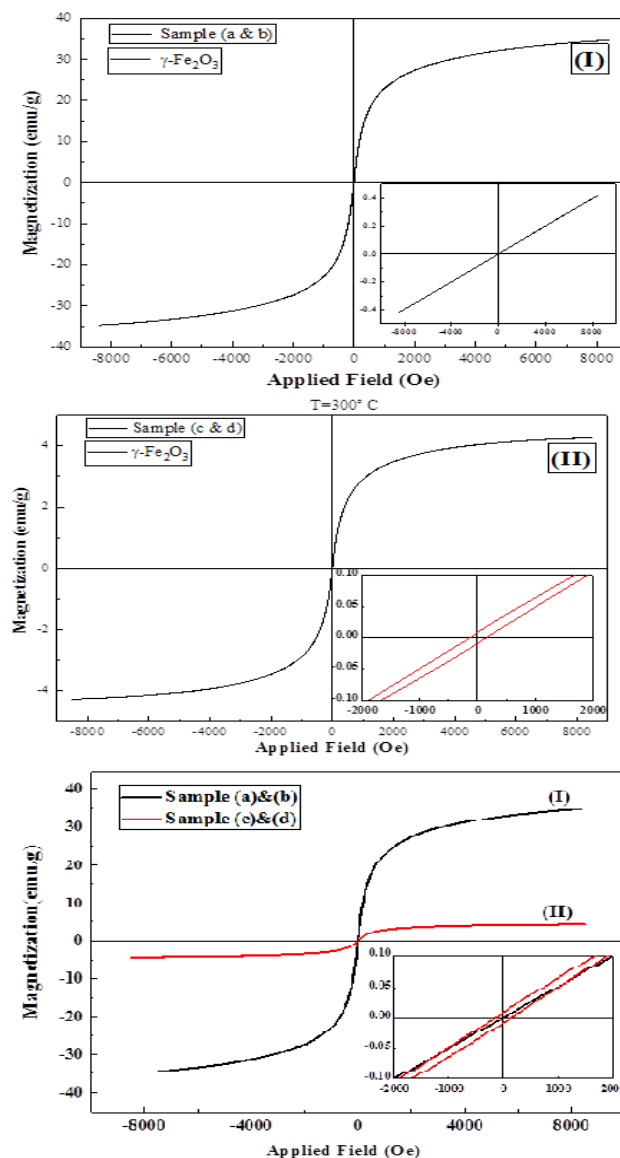


Figure 4: Magnetization curve of samples (a) and (b): (I); samples (c) and (d): (II).

Table 1: Comparison of Particle Size of Iron Oxide Nanoparticles Using XRD Analysis.

Sample Name	Size from (220)	Size from (311)	Size from (400)	Size from (422)	Size from (511)	Size from (440)	Avg. Size
Sample (a)	4 nm	2 nm	3 nm	4 nm	4 nm	8 nm	4 nm
Sample (b)	6 nm	3 nm	4 nm	4 nm	4 nm	7 nm	4.6 nm
Sample (c)	-	8 nm	-	-	-	-	-
Sample (d)	-	9 nm	-	-	-	-	-

analyses showed that the surfaces of nanoparticles were occupied by different numbers of ligands via physical absorption and chemical binding, which changes with particle size, owing to the surface area to volume ratio. The as-prepared iron oxide nanoparticles showed biocompatibility and nontoxicity against the normal as well as cancerous cell lines.

In reference²⁴ it was reported that the toxicity of nano particle was very vital and important. Furthermore our nano particles (samples a and b) in contrast of paper²⁵ of reference has less toxicity and has more magnetization and crystallization. It was shown in TEM that samples c and d in contrast of paper²⁶ of reference included smaller nano particles and smaller surface in magnetic saturation figure in analyzes. Our samples have less toxicity even in high dose of nano particles (samples d and c) and cells have more mobility for producing and growing cells.

As $\gamma\text{-Fe}_2\text{O}_3$ is a potential candidate for so many biomedical applications, such a novel magnetic structure should be of great interest.

ACKNOWLEDGMENT

The authors would like thank from: researchers in the Nano Electric Lab of Department of Physics, Faculty of Basic Sciences, University of Mazandaran, Babol-sar, Iran and Dr. Mohammad Shokrzadeh in the Pharmaceutical Sciences Research Center, Department of Clinical Pharmacy, Faculty of Pharmacy, Mazandaran University of Medical Science, Sari, Iran.

CONFLICT OF INTEREST

The author reports no conflicts of interest. The responsible for the content and writing of the article is just the author.

ABBREVIATIONS USED

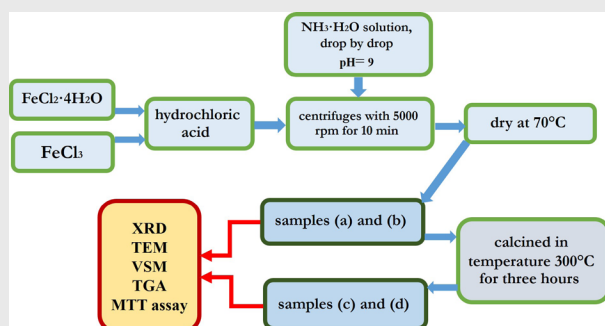
DMSO: Dimethyl Sulfoxide; **DNA:** Deoxyribonucleic acid; **ELISA reader:** Enzyme-linked immunosorbent assay; **HELA:** Henrietta Lacks (cancer cells); **LDH assay:** Lactate Dehydrogenase assay; **M-H:** Magnetic Hysteresis; **MTT assay:** Methyl Thiazolyl Tetrazolium; **NPs:** Nano Particles; **ROS:** Reactive oxygen species; **SPIONS:** Superparamagnetic Iron Oxide Nanoparticles; **TEM:** Transmission Electron Microscopy; **TGA:** Thermogravimetric Analysis; **VSM:** Vibrating Sample Magnetometer; **XRD:** X-ray Diffraction.

REFERENCES

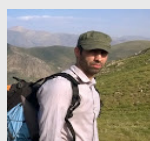
- McBain SC, Yiu HHP, Dobson J. Magnetic nanoparticles for gene and drug delivery. *International Journal of Nanomedicine* [Internet]. 2008;3(2):169-80. Available from: <http://www.ncbi.nlm.nih.gov/pmc/articles/PMC2527670/>. PMID:18686777 PMCID:PMC2527670.
- Li X, Si Z, Lei Y, Tang J, Wang S, Su S, et al. Direct hydrothermal synthesis of single-crystalline triangular Fe_3O_4 nanoprisms. *CrystEngComm* [Internet]. 2010;12(7):2060-3. Available from: <http://dx.doi.org/10.1039/B926780H>. <https://doi.org/10.1039/b926780h>.
- Kim J, Lee JE, Lee SH, Yu JH, Lee JH, Park TG, et al. Designed fabrication of a multifunctional polymer nanomedical platform for simultaneous cancer-targeted imaging and magnetically guided drug delivery. *Advanced Materials*. 2008;20(3):478-83. <https://doi.org/10.1002/adma.200701726>.
- Galloway JM, Arakaki A, Masuda F, Tanaka T, Matsunaga T, Staniland SS. Magnetic bacterial protein Mms6 controls morphology, crystallinity and magnetism of cobalt-doped magnetite nanoparticles *in vitro*. *J Mater Chem* [Internet]. 2011;21(39):15244-54. Available from: <http://dx.doi.org/10.1039/C1JM12003D> <https://doi.org/10.1039/c1jm12003d>.
- Machala L, Tuček J, Zbořil R. Polymorphous Transformations of Nanometric Iron(III) Oxide: A Review. *Chemistry of Materials* [Internet]. 2011;23(14):3255-72. Available from: <http://dx.doi.org/10.1021/cm200397g>. <https://doi.org/10.1021/cm200397g>.
- Ali K, Sarfraz a. K, Mirza IM, ul Haq a. Preparation of Superparamagnetic Maghemite ($\gamma\text{-Fe}_2\text{O}_3$) Nanoparticles by Wet Chemical Route and Investigation of Their Magnetic and Dielectric Properties. *Current Applied Physics* [Internet]. 2015;15(8):925-9. Available from: <http://linkinghub.elsevier.com/retrieve/pii/S1567173915001492>. <https://doi.org/10.1016/j.cap.2015.04.030>.
- Darezreshki E, Ranjbar M, Bakhtiari F. One-step synthesis of maghemite ($\gamma\text{-Fe}_2\text{O}_3$) nano-particles by wet chemical method. *Journal of Alloys and Compounds* [Internet]. 2010. 2015;502(1):257-60. Available from: <http://www.sciencedirect.com/science/article/pii/S0925838810010303>.
- Bhattarai SR, Kc RB, Kim SY, Sharma M, Khil MS, Hwang PH, et al. N-hexanoyl chitosan stabilized magnetic nanoparticles: Implication for cellular labeling and magnetic resonance imaging. *Journal of Nanobiotechnology* [Internet]. 2008;6:1. Available from: <http://www.ncbi.nlm.nih.gov/pmc/articles/PMC2265288/> <https://doi.org/10.1186/1477-3155-6-1> PMID:18173857 PMCID:PMC2265288.
- Kwon SG, Piao Y, Park J, Angappane S, Jo Y, Hwang N-M, et al. Kinetics of monodisperse iron oxide nanocrystal formation by "heating-up" process. *Journal of the American Chemical Society*. 2007;129(41):12571-84. <https://doi.org/10.1021/ja074633q> PMID:17887758.
- Elias A, Tsourkas A. Imaging circulating cells and lymphoid tissues with iron oxide nanoparticles. *Hematology / the Education Program of the American Society of Hematology American Society of Hematology Education Program*. 2009;720-6.
- Kok SHL, Chui CH, Lam WS, Chen J, Lau FY, Cheng GYM, et al. Apoptotic activity of a novel synthetic cantharidin analogue on hepatoma cell lines. *International journal of molecular medicine*. 2006;17(5):945-9. <https://doi.org/10.3892/ijmm.17.5.945>.
- Chui CH, Gambari R, Lau FYI, Hau DKP, Wong RSM, Cheng GYM, et al. Antiangiogenic activity of a concentrated effective microorganism fermentation extract. *International Journal of Molecular Medicine*. 2006;18(5):975-9. <https://doi.org/10.3892/ijmm.18.5.975>.

13. Shokrzadeh M, Azadbakht M, Ahangar N, Naderi H, Saeedi Saravi SS. Comparison of the cytotoxic effects of *Juniperus sabina* and *Zataria multiflora* extracts with *Taxus baccata* extract and Cisplatin on normal and cancer cell lines. *Pharmacognosy Magazine* [Internet]. 2010;6(22):102-5. Available from: <http://www.ncbi.nlm.nih.gov/pmc/articles/PMC2900055/> <https://doi.org/10.4103/0973-1296.62894> PMID:20668574 PMCID:PMC2900055.
14. Ghosh K, Chandra K, Ojha AK, Sarkar S, Islam SS. Structural identification and cytotoxic activity of a polysaccharide from the fruits of *Lagenaria siceraria* (Lau). *Carbohydrate research* [Internet]. 2009 cited 2015;344(5):693-8. Available from: <http://www.sciencedirect.com/science/article/pii/S0008621509000135>.
15. Sankari M, Chitra V, Jubilee R, Silambu Janaki P RD. Immunosuppressive activity of aqueous extract of *Lagenaria siceraria* (standley) in mice. *Pharmacia* [Internet]. 2010;2(2):208-20. Available from: <http://scholarsresearchlibrary.com/ABR-vol1-iss2/ABR-2010-1-2-87-90.pdf>
16. Abareshi M, Goharshadi EK, Mojtaba Zebarjad S, Khandan Fadafan H, Youssefi A. Fabrication, characterization and measurement of thermal conductivity of Fe_3O_4 nanofluids. *Journal of Magnetism and Magnetic Materials*. 2010;322(24):3895-901. <https://doi.org/10.1016/j.jmmm.2010.08.016>.
17. Aliahmad M, Nasiri Moghaddam N. Synthesis of maghemite ($\gamma\text{-Fe}_2\text{O}_3$) nanoparticles by thermal-decomposition of magnetite (Fe_3O_4) nanoparticles. *Materials Science-Poland* [Internet]. 2013;31(2):264-8. Available from: <http://link.springer.com/10.2478/s13536-012-0100-6> <https://doi.org/10.2478/s13536-012-0100-6>.
18. Etheridge ML, Hurley KR, Zhang J, Jeon S, Ring HL, Hogan C, *et al.* Accounting for biological aggregation in heating and imaging of magnetic nanoparticles. *Technology*. 2014;2(3):214-28. <https://doi.org/10.1142/S2339547814500198> PMID:25379513 PMCID:PMC4219565.
19. Darezreshki E. One-step synthesis of hematite ($\alpha\text{-Fe}_2\text{O}_3$) nano-particles by direct thermal-decomposition of maghemite. *Materials Letters* [Internet]. 2011;65(4):642-5. Available from: <http://www.sciencedirect.com/science/article/pii/S0167577X10009912> <https://doi.org/10.1016/j.matlet.2010.11.030>.
20. Alibeigi S, Vaezi MR. Phase Transformation of Iron Oxide Nanoparticles by Varying the Molar Ratio of $\text{Fe}_2\text{+Fe}_3\text{+}$. *Chemical Engineering & Technology* [Internet]. 2008;31(11):1591-6. Available from: <http://dx.doi.org/10.1002/ceat.200800093> <https://doi.org/10.1002/ceat.200800093>.
21. Brunner TJ, Wick P, Manser P, Spohn P, Grass RN, Limbach LK, *et al.* *In vitro* cytotoxicity of oxide nanoparticles: comparison to asbestos, silica, and the effect of particle solubility. *Environmental science & technology*. 2006;40(14):4374-81. <https://doi.org/10.1021/es052069i>.
22. Nel A, Xia T, Madler L, Li N. Toxic potential of materials at the nanolevel. *Science* (New York, NY). 2006;311(5761):622-7. <https://doi.org/10.1126/science.1114397> PMID:16456071.
23. Jeng HA, Swanson J. Toxicity of metal oxide nanoparticles in mammalian cells. *Journal of environmental science and health Part A, Toxic/hazardous substances & environmental engineering*. 2006;41(12):2699-711. <https://doi.org/10.1080/10934520600966177> PMID:17114101.
24. Singh N, Jenkins GJS, Asadi R, Doak SH. Potential toxicity of superparamagnetic iron oxide nanoparticles (SPION). *Nano Reviews*. 2010;1(0):1-5. <https://doi.org/10.3402/nano.v1i0.5358> PMID:22110864 PMCID:PMC3215220.
25. Mahmoudi M, Simchi A, Imani M, Shokrgozar MA, Milani AS, Hafeli UO, *et al.* A new approach for the *in vitro* identification of the cytotoxicity of superparamagnetic iron oxide nanoparticles. *Colloids and surfaces B, Biointerfaces*. 2010;75(1):300-9. <https://doi.org/10.1016/j.colsurfb.2009.08.044> PMID:19781921.
26. Song MM, Song WJ, Bi H, Wang J, Wu WL, Sun J, *et al.* Cytotoxicity and cellular uptake of iron nanowires. *Biomaterials* [Internet]. 2010;31(7):1509-17. Available from: <http://dx.doi.org/10.1016/j.biomaterials.2009.11.034> <https://doi.org/10.1016/j.biomaterials.2009.11.034>.

PICTORIAL ABSTRACT



About Authors



Mahdi Khodabakhshi: Masters from Department of physics, faculty of basic sciences, University of Mazandaran, Babolsar, Iran. His researches focused on the Optics, physics and nano science in biophysics, drug delivery, fuel cells and gas sensors.



Ali Bahari: Professor at the Department of physics, faculty of basic sciences, University of Mazandaran, Babolsar, Iran. His researches and articles are this: <http://ow.umz.ac.ir/en/dynamic/dynamic.asp?Userid=171>.

SUMMARY

- TEM images of iron oxide nanoparticles showed that the size of nanoparticles from 2 nm to 9 nm.
- The TG analyses showed that the surfaces of nanoparticles occupied by different numbers of ligands via physical absorption and chemical binding, which changes with particle size, owing to the surface area to volume ratio.
- As the hysteresis loops of samples a and b were 0, the magnetic nanoparticles of $\text{Fe } \gamma$ phase can correct the carrying of drugs by carrying of medicinal elements and magnetic field.
- In Figure 4 (II) for samples c and d, there was a little hysteresis so these samples can use in cancer cure with Hyperthermia therapy method. The as-prepared iron oxide nanoparticles showed biocompatibility and nontoxicity against the normal as well as cancerous cell lines.
- $\gamma\text{-Fe}_2\text{O}_3$ is a potential candidate for so many biomedical applications, such a novel magnetic structure should be of great interest.

Cite this article: Khodabakhshi M, Bahari A. Ayurvedic Liquid Dosage form *Asava* And *Arista*: An Overview. *Indian J of Pharmaceutical Education and Research*. 2017;51(2):295-301.